

1 Indomethacin Co-Crystals and Their Parent Mixtures: Does the 2 Intestinal Barrier Recognize Them Differently?

3 Valeria Ferretti,[†] Alessandro Dalpiaz,^{*,†} Valerio Bertolasi,[†] Luca Ferraro,[‡] Sarah Beggiato,[‡]
4 Federico Spizzo,[§] Enzo Spisni,^{||} and Barbara Pavan[‡]

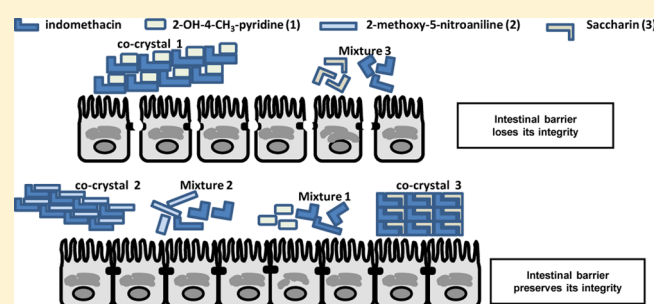
5 [†]Department of Chemical and Pharmaceutical Sciences, [‡]Department of Life Sciences and Biotechnology, and [§]Department of
6 Physics and Earth Sciences, University of Ferrara, Ferrara, Italy

7 ^{||}Department of Biological, Geological and Environmental Sciences, University of Bologna, Bologna, Italy

8 **S** Supporting Information

9 **ABSTRACT:** Co-crystals are crystalline complexes of two or
10 more molecules bound together in crystal lattices through
11 noncovalent interactions. The solubility and dissolution
12 properties of co-crystals can allow to increase the bioavail-
13 ability of poorly water-soluble active pharmaceutical ingre-
14 dients (APIs). It is currently believed that the co-crystallization
15 strategy should not induce changes on the pharmacological
16 profile of the APIs, even if it is not yet clear whether a co-
17 crystal would be defined as a physical mixture or as a new
18 chemical entity. In order to clarify these aspects, we chose
19 indomethacin as guest poorly aqueous soluble molecule and
20 compared its properties with those of its co-crystals obtained with 2-hydroxy-4-methylpyridine (co-crystal 1), 2-methoxy-5-
21 nitroaniline (co-crystal 2), and saccharine (co-crystal 3). In particular, we performed a systematic comparison among
22 indomethacin, its co-crystals, and their parent physical mixtures by evaluating via HPLC analysis the API dissolution profile, its
23 ability to permeate across intestinal cell monolayers (NCM460), and its oral bioavailability in rat. The indomethacin dissolution
24 profile was not altered by the presence of co-crystallizing agents as physical mixtures, whereas significant changes were observed
25 by the dissolution of the co-crystals. Furthermore, there was a qualitative concordance between the API dissolution patterns and
26 the relative oral bioavailabilities in rats. Co-crystal 1 induced a drastic decrease of the transepithelial electrical resistance (TEER)
27 value of NCM460 cell monolayers, whereas its parent mixture did not evidence any effect. The saccharin–indomethacin mixture
28 induced a drastic decrease of the TEER value of monolayers, whereas its parent co-crystal 3 did not induce any effects on their
29 integrity, being anyway able to increase the permeation of indomethacin. Taken together, these results demonstrate for the first
30 time different effects induced by co-crystals and their parent physical mixtures on a biologic system, findings that could raise
31 serious concerns about the use of co-crystal strategy to improve API bioavailability without performing appropriate investigations.

32 **KEYWORDS:** co-crystals, indomethacin, saccharin, drug permeation, NCM 460 cells, bioavailability



33 ■ INTRODUCTION

34 The therapeutic efficacy of a pharmaceutical formulation
35 depends on its bioavailability, i.e., the absorption extent and
36 rate of the active pharmaceutical ingredient (API) into the
37 bloodstream following its administration. The bioavailability of
38 a solid pharmaceutical formulation may depend in turn on the
39 dissolution profile of its components, in particular of the API.
40 In the case of highly lipophilic API, and therefore of a
41 compound poorly soluble in water but capable of effectively
42 permeating through biological membranes (Biopharmaceutical
43 Classification System (BCS) class II), the dissolution process is
44 the limiting factor of its absorption; in this case the
45 bioavailability is highly dependent on both dissolution rate
46 and maximum amount dissolved of the APIs themselves.¹

47 The solid state form of an API is determinant in influencing
48 its solubility and dissolution rate. In general, the amorphous
49 phases are easier to solubilize than crystalline solids, and,

among them, the metastable polymorphs can offer solubility or
dissolution advantages with respect to stable ones.^{2,3} 51

The crystal engineering of pharmaceutical solids may be very
useful to optimize the API stability and bioavailability, and the
co-crystals seem to be promising in this context.⁴ A co-crystal
can be considered as a crystalline complex of two or more
molecules bound together in the crystal lattice through
noncovalent interactions, often including hydrogen bonding.
Pharmaceutical co-crystals are obtained by an API and a co-
crystal former.⁵ It is known that the solubility and dissolution
properties of co-crystals can be similar to those of amorphous
compounds, i.e., higher than the parent crystalline pure phases. 61

Received: December 11, 2014

Revised: March 18, 2015

Accepted: March 20, 2015

62 As a consequence, pharmaceutical co-crystals give the
63 opportunities to increase bioavailability of APIs showing, at
64 the same time, the stability of their stable crystalline forms.^{6,7}

65 Currently, several APIs are known to improve their solubility
66 profile and bioavailability when co-crystallized.^{7–9} These APIs
67 include the anticonvulsant carbamazepine,¹⁰ nonsteroidal anti-
68 inflammatory drugs such as indomethacin and meloxicam,^{11,12}
69 the flavonoid quercetin,¹³ and other molecules employed as
70 model drugs.^{14–17}

71 It is currently believed that the co-crystallization strategy
72 should not induce changes in the pharmacological profile of the
73 APIs. Indeed, co-crystal design requires changes in crystal
74 structures that essentially alter hydrogen bonding motifs rather
75 than covalent bonds of the API, thus retaining its safety and
76 therapeutic properties.^{11,18} On the other hand, the regulatory
77 status regarding the use of co-crystals in pharmaceutical
78 products appears still unsettled. In particular, it is not yet
79 clear whether a co-crystal would be defined as a physical
80 mixture (enabling its classification within current compendial
81 guidelines) or as a new chemical entity requiring full safety and
82 toxicology testing.^{7,8} In this context, FDA has taken the
83 position that a co-crystal may be treated as a drug product
84 intermediate.⁸

85 In this study we evaluated the properties of (i) indomethacin,
86 chosen as guest molecule poorly soluble in aqueous environ-
87 ment,¹¹ (ii) its two new co-crystals with 2-hydroxy-4-
88 methylpyridine in its keto form (co-crystal 1) and 2-methoxy-
89 5-nitroaniline (co-crystal 2), and (iii) a previously described
90 indomethacin–saccharine co-crystal^{11,19} (co-crystal 3). The
91 schematic representation of indomethacin and the cofomers is
92 reported in Figure 1. In particular, the dissolution, the

the integrity of intestinal cell monolayers can be derived by the
dissolution of co-crystals or their parent mixtures.

■ MATERIALS AND METHODS

Materials and Reagents. γ -Indomethacin, 2-hydroxy-4-
methylpyridine, 2-methoxy-5-nitroaniline, saccharine, metha-
nol, acetonitrile, ethyl acetate, isoamyl acetate, and water were
of high performance liquid chromatography (HPLC) grade
from Sigma-Aldrich (Milan, Italy). All other reagents and
solvents were of analytical grade (Sigma-Aldrich). NCM-460
cells were kindly provided by Dr. Antonio Strillacci, University
of Bologna, Italy. The male Sprague–Dawley rats were
provided by Charles-River (Milan, Italy).

Synthesis of Adducts. Two new co-crystals containing the
indomethacin API have been synthesized and characterized by
X-ray crystallography: co-crystal 1, γ -indomethacin and 2-
hydroxy-4-methylpyridine 1:1; co-crystal 2, γ -indomethacin and
2-methoxy-5-nitroaniline 1:1. Two other co-crystals have been
synthesized and characterized but not used in the present work
because of their poor reproducibility: co-crystal a, γ -
indomethacin and 4-nitropyridine *N*-oxide monohydrate
1:1:1; co-crystal b, γ -indomethacin and pyridine *N*-oxide 1:1.
Details of the X-ray crystallographic analysis for all four crystals
are reported in Table S1 in the Supporting Information. Equi-
molar quantities of indomethacin and the co-crystal partner
were dissolved in the minimum quantity of isoamyl
acetate and left for slow evaporation at room temperature.
Crystals were observed after a few days. Co-crystal 3,
containing saccharine as the cofomer, has been obtained by
solvent slow evaporation of an equimolar saccharine/ γ -
indomethacin solution prepared according to ref 19. The
phase and composition of the co-crystals 1, 2, and 3 have been
checked by X-ray powder crystallography, comparing the
experimental spectra with those calculated from the single-
crystal crystallography structures (Figures S1–S3 in the
Supporting Information).

Experimental: X-ray. The crystallographic data for the four
co-crystals 1, 2, a, and b were collected on a Nonius Kappa
CCD diffractometer at room temperature using graphite-
monochromated Mo $K\alpha$ radiation ($\lambda = 0.71073$ Å). Data sets
were integrated with the Denzo-SM package²⁰ and corrected
for Lorentz-polarization effects. The structures were solved by
direct methods with the SIR97 suite of programs,²¹ and
refinement was performed on F^2 by full-matrix least-squares
methods with all non-hydrogen atoms anisotropic. The N/O–
H atoms were found in the difference Fourier map and refined
isotropically; all other hydrogen atoms were included on
calculated positions, riding on their carrier atoms. All
calculations were performed using SHELXL-97²² implemented
in the WINGX system of programs.²³ The ORTEPIII²⁴
diagrams of co-crystals 1 and 2 are shown in Figure 2. Powder
diffraction spectra for co-crystals 1, 2, and 3 were recorded,
at room temperature, on a Bruker D-8 Advance diffractometer
with graphite monochromatized Cu $K\alpha$ radiation ($\lambda = 1.5406$
Å). The data were recorded at 2θ steps of 0.02° with 1 s/step.
Crystallographic data for the structural analysis of the four new
compounds have been deposited at the Cambridge Crystallo-
graphic Data Center, 12 Union Road, Cambridge, CB2 1EZ,
U.K., and are available free of charge from the Director on
request quoting the deposition number CCDC 1005832–
1005835 for 1, 2, a, and b, respectively.

Differential Scanning Calorimetry (DSC). Thermal
analyses on the samples were performed on a PerkinElmer

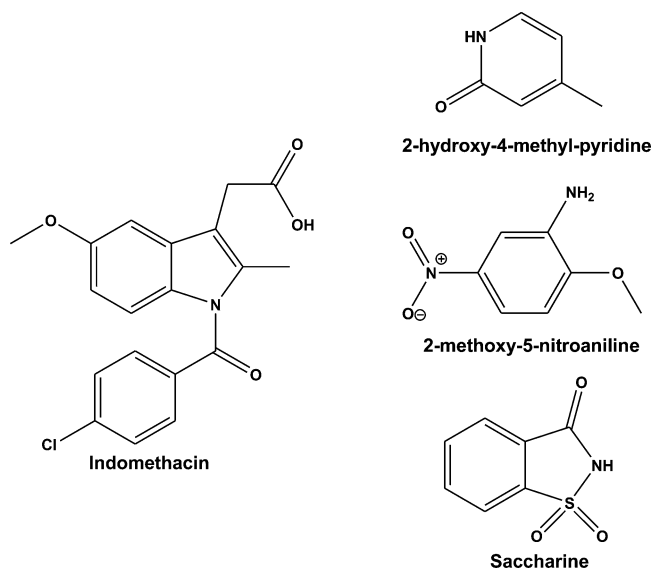


Figure 1. Schematic representation of indomethacin and the cofomers 2-hydroxy-4-methylpyridine in its keto form, 2-methoxy-5-nitroaniline, and saccharine in co-crystals 1, 2, and 3, respectively.

93 permeation across NCM460 cell monolayers employed as an
94 *in vitro* model of human intestinal epithelial barrier, and the
95 bioavailability after oral administration to rats of indomethacin,
96 its co-crystals, and their parent mixtures (1, 2 and 3,
97 respectively) have been investigated. Overall, the results
98 indicate, for the first time, that strongly different effects on

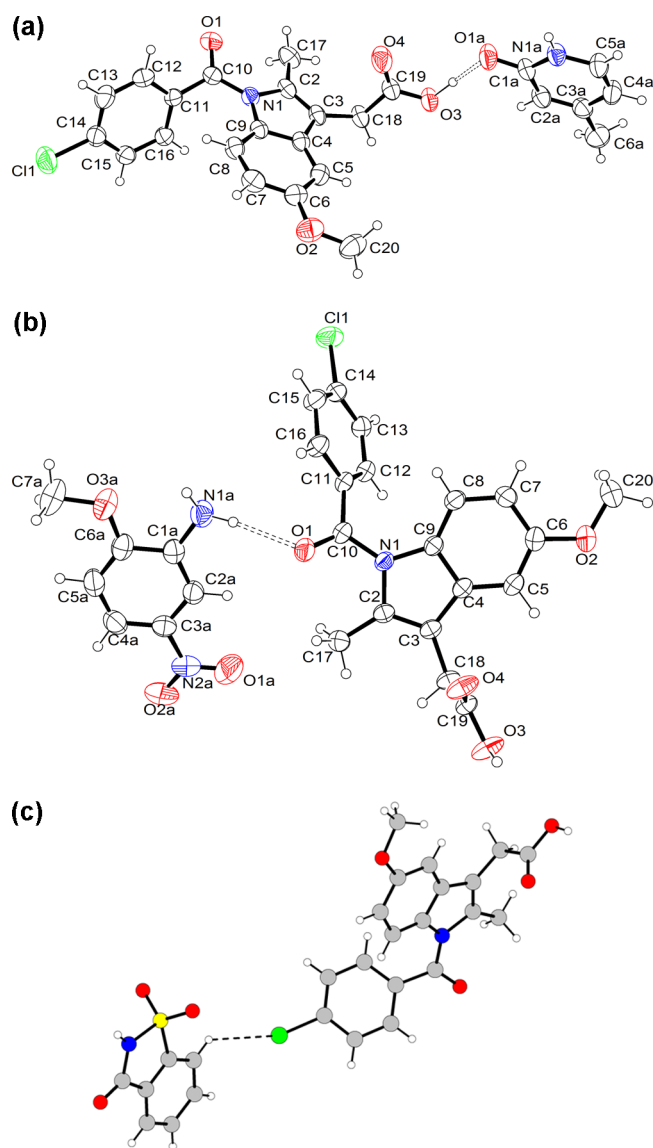


Figure 2. (a) ORTEPIII view and atom numbering scheme for co-crystals 1. (b) ORTEPIII view and atom numbering scheme for co-crystals 2. (c) Indomethacin-saccharine complex 3 (from ref 19). Thermal ellipsoids are drawn at the 40% probability level. Hydrogen bonds are drawn as dashed lines.

161 differential scanning calorimeter DSC7; temperature and heat
162 calibration were done using indium and zinc standards. The
163 samples (4–6 mg) were put in nonhermetic aluminum pans
164 and scanned at a heating rate of 10 °C/min in the 30–300 °C
165 range under a continuous purged dry nitrogen atmosphere. The
166 data were collected in triplicate for each sample.

167 **HPLC Analysis.** The quantification of the indomethacin was
168 performed by HPLC. The chromatographic apparatus consisted
169 of a modular system (model LC-10 AD VD pump and model
170 SPD-10A VP variable wavelength UV-vis detector; Shimadzu,
171 Kyoto, Japan) and an injection valve with 20 μ L sample loop
172 (model 7725; Rheodyne, IDEX, Torrance, CA, USA).
173 Separation was performed at room temperature on a reverse
174 phase column Hypersil BDS C-18, 5 μ , equipped with a guard
175 column packed with the same Hypersil material (Alltech Italia
176 Srl BV, Milan, Italy). Data acquisition and processing were
177 accomplished with a personal computer using CLASS-VP
178 Software, version 7.2.1 (Shimadzu Italia, Milan, Italy). The

169 detector was set at 319 nm. The mobile phase consisted of a
170 mixture of methanol and 0.2 phosphoric acid (75:25 v/v). The
171 flow rate was 1 mL/min. The compound 9-phenylcarbazole was
172 employed as internal standard in extraction procedures of
173 indomethacin from rat blood (see below). The retention times
174 for indomethacin and 9-phenylcarbazole were 4.0 and 13.5 min,
175 respectively.

176 The chromatographic precision for each compound was
177 evaluated by repeated analysis ($n = 6$) of the same samples (100
178 μ M). For indomethacin and 9-phenylcarbazole (employed as
179 internal standard in the extraction procedures) dissolved in
180 aqueous phase the values were obtained for 100 μ M (0.036
181 mg/mL) solutions and were represented by the relative
182 standard deviation (RSD) values ranging between 0.63% and
183 0.74%, respectively.

184 The calibration curves of indomethacin dissolved in
185 phosphate buffer 200 mM and in PBS 10 mM were linear
186 over the ranges of 50 μ M (0.018 mg/mL) to 1500 μ M (0.54
187 mg/mL) and 2 μ M (0.00072 mg/mL) to 500 μ M (0.18 mg/
188 mL), respectively ($n = 8$, $r > 0.997$, $P < 0.0001$). The limit of
189 quantification for indomethacin was 625 nM (224 ng/mL, 2.24
190 ng injected) with a signal-to-noise ratio of 10, whereas the limit
191 of detection was 188 nM (67 ng/mL, 0.67 ng injected) with a
192 signal-to-noise ratio of 3.

193 A preliminary analysis performed with 100 μ M solutions
194 showed that hydroxy-4-methylpyridine, 2-methoxy-5-nitroani-
195 line, and saccharin did not interfere with the indomethacin and
196 9-phenylcarbazone retention times.

197 **Dissolution Studies.** For the dissolution studies, the
198 samples were micronized and sieved using stainless steel
199 standard-mesh sieves (mesh size 106 μ m). In each experiment,
200 the solid powders were added to 12 mL of phosphate buffer
201 200 mM and incubated at 37 °C under gentle shaking (100
202 rpm) in a water bath. The amounts of sieved samples added to
203 the buffer solution were 57.6 mg of indomethacin; 75.2 mg of
204 co-crystal 1; 84.7 mg of co-crystal 2; 86.9 mg of co-crystal 3;
205 57.6 mg of indomethacin mixed with 17.6 mg of 2-hydroxy-4-
206 methylpyridine, 27.1 mg of 2-methoxy-5-nitroaniline, or 29.3
207 mg of saccharin for mixtures 1, 2, or 3, respectively. Aliquots
208 (200 μ L) were withdrawn from the resulting slurry at fixed time
209 intervals and filtered through regenerated cellulose filters (0.45
210 μ m). The resulting filtered samples were diluted 1:10 in water,
211 and then 10 μ L was injected into the HPLC system in order to
212 quantify the indomethacin concentrations.

213 Dissolution experiments were conducted also in PBS 10 mM
214 at 37 °C with the same procedure as described above, with the
215 only difference that the filtered samples obtained from the
216 slurry of mixture 3 were not diluted 1:10, but directly injected
217 into the HPLC system. All the values obtained were the mean
218 of three independent experiments.

219 **Cell Culture.** The NCM460 cell line was grown in DMEM
220 + Glutamax supplemented with 10% fetal bovine serum (FBS),
221 100 U/mL penicillin, and 100 g/mL streptomycin at 37 °C in a
222 humidified atmosphere of 95%, with 5% of CO₂. For maximum
223 viability, NCM460 cells were subcultured in fresh and spent
224 growth medium in 1:1 ratio. All cell culture reagents were
225 provided by Invitrogen (Life Technologies, Milan, Italy).

226 **Differentiation of NCM460 Cells to Polarized Mono-
227 layers.** Differentiation to NCM460 cell monolayers was
228 performed modifying the method reported by Dalpiaz and
229 co-workers.²⁵ Briefly, after two passages, confluent NCM460
230 cells were seeded at a density of 10⁵ cells/mL in a 1:1 ratio of
231 fresh and spent culture medium in 12-well Millicell inserts 240

242 (Millipore, Milan, Italy) consisting of 1.0 μm pore size
 243 polyethylene terephthalate (PET) filter membranes, whose
 244 surface was 1.12 cm^2 . Filters were presoaked for 24 h with fresh
 245 culture medium, and then the upper compartment (apical, A)
 246 received 400 μL of the diluted cells, whereas the lower
 247 (basolateral, B) received 2 mL of the medium in the absence of
 248 cells. Half volume of the culture medium was replaced every 2
 249 days with fresh medium to each of the apical and basolateral
 250 compartments. The integrity of the cell monolayers was
 251 monitored by measuring the transepithelial electrical resistance
 252 (TEER) by means of a voltmeter (Millicell-ERS; Millipore,
 253 Milan, Italy). The measured resistance value was multiplied by
 254 the area of the filter to obtain an absolute value of TEER,
 255 expressed as $\Omega\cdot\text{cm}^2$. The background resistance of blank inserts
 256 not plated with cells was around 35 $\Omega\cdot\text{cm}^2$ and was deducted
 257 from each value. The homogeneity and integrity of the cell
 258 monolayer were also monitored by phase contrast microscopy.
 259 Based on these parameters, cell monolayers reached confluence
 260 and epithelial polarization after 6 days, and monolayers with
 261 TEER stable value around 180 $\Omega\cdot\text{cm}^2$ were used for permeation
 262 studies. At this time, the medium was replaced with low serum
 263 fresh medium (1% FBS) in both the apical and basal
 264 compartments.

265 **Permeation Studies across Cell Monolayers.** For
 266 permeation studies, inserts were washed twice with prewarmed
 267 PBS buffer in the apical (A, 400 μL) and basolateral (B, 2 mL)
 268 compartments, and then PBS buffer containing 5 mM glucose
 269 at 37 $^\circ\text{C}$ was added to the apical compartment. The sieved
 270 powders (mesh size 106 μm) were added to the apical
 271 compartments in the following amounts: 1.92 mg of
 272 indomethacin; 2.5 mg of co-crystal 1; 2.8 mg of co-crystal 2;
 273 2.9 mg of co-crystal 3; 1.92 mg of indomethacin mixed with
 274 0.59 mg of 2-hydroxy-4-methylpyridine, or 0.90 mg of 2-
 275 methoxy-5-nitroaniline, or 0.98 mg of saccharin for mixtures 1,
 276 2, or 3, respectively. During permeation experiments, Millicell
 277 inserts loaded with the powders were continuously swirled on
 278 an orbital shaker (100 rpm; model 711/CT, ASAL, Cernusco,
 279 Milan, Italy) at 37 $^\circ\text{C}$. At programmed time points the inserts
 280 were removed and transferred into the subsequent wells
 281 containing fresh PBS, and then basolateral PBS was harvested,
 282 filtered through regenerated cellulose filters (0.45 μm), and
 283 injected (10 μL) into the HPLC system for the determination
 284 of the concentration of indomethacin.

285 At the end of incubation the apical slurries were withdrawn,
 286 filtered, and injected into the HPLC system (10 μL) after 1:10
 287 dilution, with the exception of the apical sample of the mixture
 288 3, which was directly injected after filtration, without dilution.
 289 After the withdrawal of apical samples, 400 μL of PBS was
 290 inserted in the apical compartments and TEER measurements
 291 were performed.

292 Permeation experiments were also conducted using cell-free
 293 inserts in the same conditions described above. All the values
 294 obtained were the mean of three independent experiments.

295 Apparent permeability coefficients (P_{app}) of indomethacin
 296 were calculated according to the following equation:^{26–28}

$$297 \quad P_{\text{app}} = \frac{dc}{dt} \frac{V_r}{S_A C} \quad (1)$$

298 where P_{app} is the apparent permeability coefficient in cm/min ;
 299 dc/dt is the flux of drug across the filters, calculated as the
 300 linearly regressed slope through linear data; V_r is the volume in
 301 the receiving compartment (basolateral = 2 mL); S_A is the

diffusion area (1.13 cm^2); and C is the compound
 concentration in the donor chamber (apical) detected at 60
 min and chosen as approximate apical concentration.

Statistical Analysis about Permeation Studies. Stat-
 istical comparisons between apparent permeability coefficients
 or between apical concentrations of indomethacin were
 performed by one way ANOVA followed by Dunnett's post-
 test; statistical comparisons between transepithelial electrical
 resistance before and after incubation with the sieved samples
 was performed by one way ANOVA followed by Bonferroni
 post-test. $P < 0.001$ was considered statistically significant. All
 the calculations were performed by using the computer
 program Graph Pad Prism (GraphPad Software Incorporated,
 La Jolla, CA, USA), which was employed also for the linear
 regression of the cumulative amounts of the compounds in the
 basolateral compartments of the Millicell systems. The quality
 of fit was determined by evaluating the correlation coefficients
 (r) and P values.

**In Vivo Administration of Indomethacin: Intravenous
 Infusion.** Male Sprague–Dawley rats (200–250 g) kept fasting
 since 24 h received a femoral intravenous infusion of 0.90 mg/
 mL indomethacin dissolved in a medium constituted by 20%
 (v/v) DMSO and 80% (v/v) physiologic solution, with a rate of
 0.2 mL/min for 5 min. Four rats were employed for femoral
 intravenous infusions. At the end of infusion and at fixed time
 points within 24 h, blood samples (300 μL) were collected and
 inserted in heparinized test tubes, which were centrifuged at 4
 $^\circ\text{C}$ for 15 min at 1500g; 100 μL of plasma was then withdrawn
 and immediately quenched in 300 μL of ethanol (4 $^\circ\text{C}$); 100
 μL of internal standard (100 μM 9-phenylcarbazole dissolved in
 ethanol) was then added. After centrifugation at 13000g for 10
 min, 400 μL aliquots were reduced to dryness under a nitrogen
 stream and stored at -20 $^\circ\text{C}$ until analysis. The samples were
 dissolved in 150 μL of mobile phase (methanol and 0.2
 phosphoric acid 75:25 v/v), and, after centrifugation, 10 μL was
 injected into the HPLC system for indomethacin assay. All the
 values obtained were the mean of four independent experi-
 ments.

The efficacy of indomethacin extraction from blood samples
 was determined by recovery experiments, comparing the peak
 areas extracted from 10 μM (3.58 $\mu\text{g}/\text{mL}$) blood test samples
 at 4 $^\circ\text{C}$ with those obtained by injection of an equivalent
 concentration of the drug dissolved in their mobile phase. The
 average recovery \pm SD of indomethacin from rat blood resulted
 87.4 \pm 3.9%. The concentrations of this compound were
 therefore referred to as peak area ratio with respect to the
 internal standard 9-phenylcarbazole. The precision of the
 method based on peak area ratio, calculated for 10 μM (3.6
 $\mu\text{g}/\text{mL}$) solutions, was represented by RSD values of 0.93%. The
 calibration of indomethacin was performed by employing eight
 different concentrations in whole blood at 4 $^\circ\text{C}$ ranging from 2
 μM (0.72 $\mu\text{g}/\text{mL}$) to 50 μM (18.0 $\mu\text{g}/\text{mL}$) and expressed as
 peak area ratios of the compounds to the internal standard
 versus concentration. The calibration curve resulted as linear (n
 = 8, $r = 0.990$, $P < 0.0001$). The accuracy of the extraction
 method was determined with respect to the calibration curve
 and was described by relative errors comprised between
 -2.63% and 0.24%.

The *in vivo* half-life of indomethacin in the blood was 360
 calculated by nonlinear regression (exponential decay) of 361
 concentration values in the time range within 24 h after 362
 infusion and confirmed by linear regression of the log 363
 concentration values versus time. The area under the 364

365 concentration–time curve (AUC) value was calculated by the
 366 trapezoidal method within 24 h, and the remaining area was
 367 determined as the ratio between the indomethacin concen-
 368 tration detected at 24 h and the elimination constant (k_{el}),
 369 which was obtained from the slope of the semilogarithmic plot
 370 ($-\text{slope} \times 2.3$). All the calculations were performed by using
 371 the computer program Graph Pad Prism.

372 *In Vivo* Administration: Oral Administration of 373 Indomethacin, Its Co-Crystals, and Its Parent Mixtures.

374 The sieved powders were mixed with palatable food in order to
 375 induce their oral assumption by male Sprague–Dawley rats
 376 (200–250 g) kept fasting since 24 h. The following doses were
 377 administered: 0.90 mg of indomethacin; 1.18 mg of co-crystal
 378 1; 1.32 mg of co-crystal 2; 1.36 mg of co-crystal 3; 0.90 mg of
 379 indomethacin mixed with 0.28 mg of 2-hydroxy-4-methylpyr-
 380 idine, or 0.42 mg of 2-methoxy-5-nitroaniline, or 0.46 mg of
 381 saccharin for mixtures 1, 2, or 3, respectively. Four rats/group
 382 were employed for the oral administration experiments. At the
 383 end of administration and at fixed time points within 24 h,
 384 blood samples (300 μL) were collected, then extracted, and
 385 analyzed as described above. All the concentration values
 386 obtained for indomethacin were the mean of four independent
 387 experiments. The AUC values referred to each orally
 388 administered treatment were calculated as described above.
 389 The absolute bioavailability values of indomethacin, referred to
 390 the oral administered samples, were obtained as the ratio
 391 between their oral AUC values and the AUC of the intravenous
 392 administration of the drug. All the calculations were performed
 393 by using the computer program Graph Pad Prism.

394 **Statistical Analysis about *in Vivo* Administration of
 395 Indomethacin.** Statistical comparisons between absolute
 396 bioavailability values were performed by one way ANOVA
 397 followed by Dunnett's post-test. $P < 0.001$ was considered
 398 statistically significant. All the calculations were performed by
 399 using the computer program Graph Pad Prism.

400 ■ RESULTS

401 **Indomethacin Co-Crystals.** Indomethacin was co-crystal-
 402 lized with two model molecules, 2-hydroxy-4-methylpyridine in
 403 its keto form (co-crystal 1) and 2-methoxy-5-nitroaniline (co-
 404 crystal 2). Their chemical structures along with that of the
 405 previously reported^{11,19} indomethacin–saccharin co-crystal
 406 (co-crystal 3) are reported in Figure 1. The X-ray three-
 407 dimensional structures for the three co-crystals are shown in
 408 Figure 2, which evidences that the covalent bonds of each single
 409 molecule are not altered in the co-crystallized structures and
 410 shows the main hydrogen bonding interactions between
 411 indomethacin and co-crystallizing agents (dashed lines). In 1,
 412 the pyridine derivatives are linked in dimers by N1A–H \cdots O1A
 413 hydrogen bonds (Table S3 of the Supporting Information) and
 414 each dimer, in turn, is linked on both sides to two
 415 indomethacin molecules through O3–H \cdots O1A hydrogen
 416 bonds involving the indomethacin carboxylic group (Figure
 417 2a). In 2, the indomethacin molecules are coupled in dimeric
 418 units by O3–H \cdots O4 hydrogen bonds, as found in the crystal
 419 lattice of the pure γ -indomethacin crystal.²⁹ The dimers link the
 420 cofomer molecules through the O1 chetonic oxygen, forming
 421 N–H \cdots O interactions of medium strength (Figure 2b). In 3,
 422 the indomethacin and saccharin molecules form in the crystal
 423 carboxylic acid and imide centrosymmetric dimers, respectively,
 424 resembling the arrangements found in the pure crystals.^{29,30}
 425 The different dimers interact via a number of weak C–H \cdots O/
 426 Cl interactions; the most relevant of them is shown in Figure 2c

(C \cdots Cl distance: 3.54 Å). More details about the crystal
 structures and the packing arrangements can be found in the
 Supporting Information.

DSC Analysis. The DSC traces and thermal data for γ -
 indomethacin and its co-crystals are presented in Figure 3.

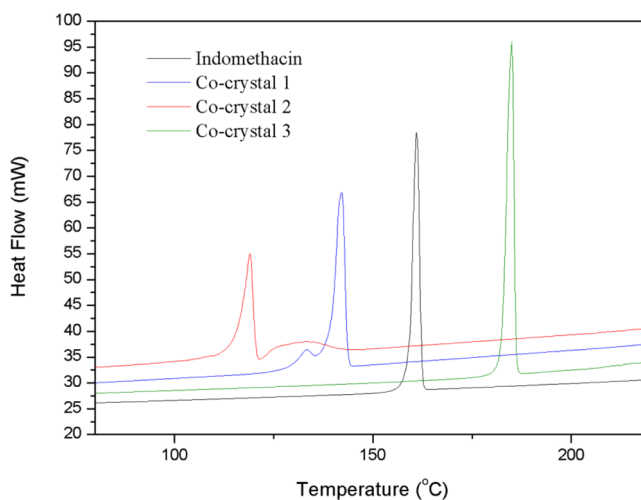


Figure 3. DSC thermograms for indomethacin and its co-crystals.

Indomethacin showed a single melting transition with T_{max}
 $= 160.8$ °C and enthalpy (ΔH_f) = 38.42 kJ/mol (Figure 3 and
 Table 1). The DSC thermogram for co-crystals 1, 2, and 3

Table 1. Melting Points and Enthalpy Values for γ -
 Indomethacin and Its Co-Crystals^a

compound	melting point (°C)	ΔH (kJ/mol)
γ -indomethacin	160.8 \pm 0.8	38.42 \pm 0.11
co-crystal 1	141.7 \pm 0.3	66.16 \pm 0.14
co-crystal 2	118.9 \pm 0.3	55.75 \pm 1.05
co-crystal 3	184.6 \pm 0.4	77.46 \pm 0.81

^aData are reported as mean \pm SD of three independent experiments.

showed marked endothermic transitions attributed to the
 melting transition at $T_{\text{max}} = 141.7$, 118.9, and 184.6 °C,
 respectively (Figure 3 and Table 1). The related ΔH_f values
 were 66.16 kJ/mol for co-crystal 1, 55.75 kJ/mol for co-crystal
 2, and 77.46 kJ/mol for co-crystal 3.

**Dissolution Studies. Co-Crystals Can Significantly
 Change the Dissolution Profiles of Indomethacin.** Figure
 4A reports a comparison between the dissolution profiles in
 200 mM phosphate buffer at 37 °C of γ -indomethacin, as free
 drug, co-crystallized, or mixed in the parent mixtures. The
 saturation concentration of free γ -indomethacin, reached after
 about 2 h of its incubation in the buffer, was about 1.8 mg/mL.
 The dissolution profile of γ -indomethacin was not altered by
 the presence of the co-crystallizing agents when mixed with the
 drug. Differently, the co-crystallized powders induced signifi-
 cant changes of indomethacin dissolution profiles. In particular,
 the co-crystal 1 and the co-crystal 2 induced an increase up to
 three times and a 50% decrease of γ -indomethacin saturation
 concentration, respectively, without affecting the dissolution
 rate. Finally, the co-crystal 3 induced not only a significant
 enhancement of the saturation concentration of γ -indomethacin
 (up to four times) but, differently from the other co-crystals,

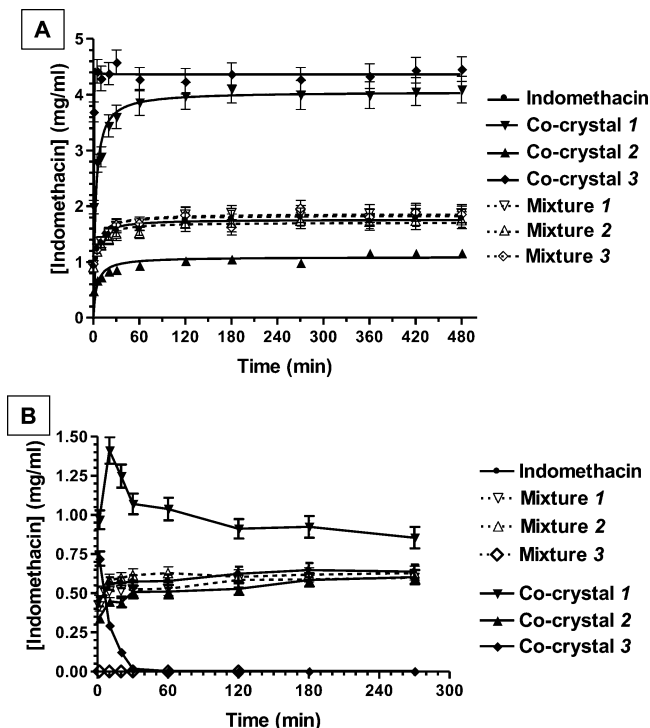


Figure 4. Solubility and dissolution profiles in phosphate buffer 200 mM (A) and PBS 10 mM (B) at 37 °C for γ -indomethacin as free drug, or co-crystallized, or mixed in the parent mixtures. Data are reported as the mean \pm SD of three independent experiments.

also an increase of the drug dissolution rate, 30 min being the time necessary to reach the saturation conditions.

The indomethacin solubility and dissolution profiles represented in Figure 4A drastically changed when the powders were incubated in PBS 10 mM, the medium employed for the drug permeation studies across NCM460 cell monolayers (see below). In particular, under these experimental conditions, the saturation concentration of free γ -indomethacin was reduced of about 50% when compared to that measured when it was dissolved in 200 mM phosphate buffer (Figure 4B); the mixtures 1 and 2 showed dissolution profiles similar to that of free γ -indomethacin, whereas the mixture 3 induced a drastic decrease of the saturation concentration of the drug, showing a mean \pm SD value of 0.0012 ± 0.0004 mg/mL (about 0.2% of the saturation concentration of the free drug). The co-crystal 1 was instead associated with an increase of indomethacin saturation concentration. Differently from the results obtained under 200 mM phosphate buffer conditions (see above), the co-crystal 2 led to an indomethacin dissolution profile similar to those displayed by the free drug. Finally, the co-crystal 3 induced a very fast dissolution of indomethacin that was, however, followed by a sudden precipitation of the drug; this event was completed within 60 min, showing indomethacin concentration values about 0.003 mg/mL.

Permeation Studies. Co-Crystals Can Induce Different Effects on Cell Monolayers with Respect to Their Parent Mixtures. The PBS was used as incubation medium for the permeation studies of indomethacin across an *in vitro* model of human intestinal wall, i.e., NCM460 cell monolayers.³¹ In order to simulate an oral administration, the powders of γ -indomethacin, its co-crystals, or the parent mixtures were introduced in the apical compartment of the “Millicell” systems with the same ratio between solid powders and incubation

medium adopted for dissolution studies. The indomethacin permeation profiles, expressed by the cumulative concentrations in the receiving basolateral compartments, are reported in Figure 5. The linear profiles indicate constant permeation

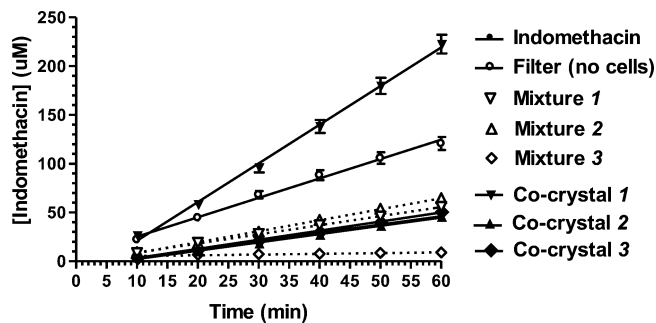


Figure 5. Permeation kinetics of indomethacin after introduction in the “Millicell” apical compartments of powders constituted by free γ -indomethacin, its co-crystals, or the parent mixtures of γ -indomethacin with co-crystallizing agents. The permeations were analyzed across monolayers obtained by NCM460 cells. The permeation of free γ -indomethacin was analyzed across the Millicell filters alone (filter) or coated by monolayers. The cumulative amounts in the basolateral receiving compartments were linear within 60 min ($r \geq 0.97$, $P \leq 0.001$). The resulting slopes of the linear fits were used for the calculation of permeability coefficients (P_{app}). All data are reported as mean \pm SD of three independent experiments.

conditions during the analysis time period (60 min) for all samples. The straight line related to mixture 3 ($r = 0.970$, $P = 0.001$) was characterized by indomethacin concentration values strongly lower than those of the straight lines of the other powders ($r \geq 0.998$, $P < 0.0001$). The apparent permeability coefficients (P_{app}) of indomethacin (Table 2) have been calculated on the basis of the resulting slopes of the linear fits and the indomethacin concentrations detected in the apical compartments after 1 h of incubation of the powders (Table 2), chosen as approximate apical concentrations. These latter values appeared essentially in line with those obtained from dissolution studies of indomethacin powders in 10 mM PBS (Figure 4B). Indeed, the drug concentrations obtained from the powders constituted by γ -indomethacin, mixtures 1 and 2, and co-crystal 2 were not statistically dissimilar among them (about 1000 μ M, $P > 0.05$). On the other hand, mixture 3 induced a drastic reduction of indomethacin concentration ($P < 0.001$), showing values close to the drug limit of quantification. Furthermore, the co-crystal 1 induced an increase of indomethacin concentration of about three times with respect to the free drug powder ($P < 0.001$), whereas the co-crystal 3 significantly reduced the γ -indomethacin concentration ($P < 0.001$), even in a less drastic manner than detected from dissolution experiments in 10 mM PBS in the absence of cells (Figure 4B). Indeed, as reported in Table 2, the apical concentration of indomethacin dissolved at 60 min from co-crystal 3 was about 440 μ M, with a pH value of 5.5, whereas in dissolution experiments (without cells) it was about 10 μ M with a pH value of 3.2. The same pH values were registered at 60 min for dissolution of mixture 3 in the presence and in the absence of cells, respectively. These data, therefore, confirm the aptitude of co-crystal 3 to enhance the indomethacin dissolution pattern with respect to its parent physical mixture. Indeed, a less acid pH value induced by the presence of cells allowed co-crystal 3 to enhance the amounts of indomethacin

Table 2. Data Related to Indomethacin *in Vitro* Dissolution and Permeation Studies and *in Vivo* Oral Bioavailability^a

powder	permeation condition	solubility in PBS 10 mM at 60 min (μM)	apical concns at 60 min (μM)	P_{app} ($\times 10^{-5}$ cm/min)	TEER ($\Omega\cdot\text{cm}^2$)		absolute bioavailability (%)
					0 min	60 min	
γ -indomethacin	cells	1612 \pm 84	1010 \pm 40	150 \pm 6	181 \pm 10	163 \pm 8	23.5 \pm 0.8
mixture 1	cells	1475 \pm 90	989 \pm 42	165 \pm 7	181 \pm 9	158 \pm 7	25.7 \pm 1.6
co-crystal 1	cells	2900 \pm 138*	2708 \pm 84*	301 \pm 14*	185 \pm 11	21 \pm 1**	37.7 \pm 1.5***
mixture 2	cells	1755 \pm 96	1047 \pm 50	147 \pm 10	183 \pm 10	152 \pm 7	24.4 \pm 1.2
co-crystal 2	cells	1426 \pm 88	1013 \pm 38	145 \pm 6	177 \pm 9	159 \pm 8	20.1 \pm 0.9***
mixture 3	cells	2.3 \pm 0.3*	3.2 \pm 0.1*		180 \pm 10	36 \pm 2**	24.8 \pm 0.9
co-crystal 3	cells	10.4 \pm 0.8*	442 \pm 18*	374 \pm 16*	183 \pm 10	164 \pm 8	33.6 \pm 0.6***
γ -indomethacin	filter		1015 \pm 45	429 \pm 18*			

^aPermeation studies were performed by using “Millicell” filters alone (filter) or coated by NCM460 cell monolayers (cells). Indomethacin was introduced in the donor compartment as sieved powder of γ -indomethacin, or its co-crystals, or the parent mixtures. The apical concentrations detected at the end of incubation were employed for the calculation of the apparent permeation coefficients (P_{app}). Permeation studies were performed after cell cultures reached the confluence using parallel sets of “Millicell” well plates with similar TEER values (TEER 0 min). The TEER values were measured again at the end of incubation (TEER 60 min). All data related to permeation studies are reported as the mean \pm SD of three independent experiments. Bioavailability data were obtained after oral administration to rats of the powders and are reported as the mean \pm SD of four independent experiments. * $P < 0.001$ versus γ -indomethacin corresponding value. ** $P < 0.001$ versus TEER at “time 0” (0 min). *** $P < 0.001$ versus absolute bioavailability of γ -indomethacin.

529 dissolved in the medium. The dissolution of all other powders
530 analyzed appeared slightly influenced by the presence of the
531 cells (Table 2). The pH values of dissolution media of these
532 powders at 60 min ranged from 7.0 to 7.5 both in the presence
533 and in the absence of cells. The slope of the permeation profile
534 (Figure 5) and the apical concentration of indomethacin related
535 to mixture 3 (Table 2) appeared too low to obtain a reliable
536 P_{app} value of indomethacin dissolved from this sample.

537 A comparison of the P_{app} values of γ -indomethacin (Table 2)
538 obtained in the presence ($150 \times 10^{-5} \pm 6 \times 10^{-5}$ cm/min) and
539 in the absence ($429 \times 10^{-5} \pm 18 \times 10^{-5}$ cm/min) of NCM460
540 cell monolayers indicated a significantly lower permeation of
541 the drug in the presence of cells ($P < 0.001$), confirming the
542 validity of the monolayer as an *in vitro* model of a physiologic
543 barrier. This behavior appeared in agreement with the
544 transepithelial electrical resistance (TEER) values (about 180
545 $\Omega\cdot\text{cm}^2$) attributed to the monolayers before their incubation
546 with the powders (Table 2). The apparent coefficient values
547 across the monolayer of indomethacin dissolved from mixtures
548 1 and 2 and co-crystal 2 did not significantly differ from the P_{app}
549 obtained for the free γ -indomethacin (Table 2, $P > 0.05$). On
550 the other hand, the co-crystal 1 induced a consistent increase of
551 indomethacin permeation ($P_{\text{app}} = 301 \times 10^{-5} \pm 11 \times 10^{-5}$ cm/
552 min, $P < 0.001$). This phenomenon was associated with the
553 ability of this co-crystal to impair the tight junctions among the
554 cells of the monolayer. This ability was evidenced by the drastic
555 reduction of TEER values ($P < 0.001$) measured after 60 min of
556 incubation with this sample ($21 \pm 1 \Omega\cdot\text{cm}^2$) in comparison to
557 the value obtained before incubation (185 ± 11). Moreover,
558 monitoring the monolayer after its incubation with co-crystal 1
559 by phase contrast microscopy evidenced a complete separation
560 of the cells (data not shown). It is remarkable that mixture 1
561 incubation altered neither the monolayer integrity, as
562 monitored by phase contrast microscopy (data not shown),
563 nor the TEER value (before incubation = $181 \pm 9 \Omega\cdot\text{cm}^2$; after
564 incubation = $158 \pm 7 \Omega\cdot\text{cm}^2$; $P > 0.05$). The same profile has
565 been also registered for the powder of free γ -indomethacin, the
566 mixture 2, and the co-crystals 2 and 3. It is interesting to
567 observe that the mixture 3 induced a cell monolayer
568 fragmentation, as monitored by phase contrast microscopy
569 (data not shown) and indicated by the TEER value (before
570 incubation = $180 \pm 10 \Omega\cdot\text{cm}^2$; after incubation = $36 \pm 2 \Omega\cdot$

571 cm^2 ; $P < 0.001$). The co-crystal 3 has been characterized by a
572 P_{app} value of $374 \times 10^{-5} \pm 16 \times 10^{-5}$ cm/min, significantly
573 higher with respect to that obtained with the powder of free γ -
574 indomethacin ($P < 0.001$). Interestingly, the permeation
575 enhancement induced by co-crystal 3 was not related to the
576 monolayer fragmentation (data not shown).

***In Vivo* Administration of Indomethacin: Its Oral Bioavailability Is Modulated by Co-Crystallization.** After
577 intravenous infusion of 0.90 mg indomethacin, the drug
578 concentration in the rat bloodstream was $13.2 \pm 1.4 \mu\text{g}/\text{mL}$.
579 This value decreased during time with an apparent first order
580 kinetic (Figure 6A) confirmed by the linearity of the
581 semilogarithmic plot reported in the inset of Figure 6A ($n =$
582 8, $r = 0.983$, $P < 0.0001$), showing a half-life value of $8.94 \pm$
583 0.38 h.
584

585 The rat blood indomethacin concentrations within 24 h after
586 its intravenous infusion (iv) as free drug or the oral
587 administration of 0.90 mg of indomethacin as sieved powders
588 of free γ -drug, its co-crystals, and the parent mixtures are
589 reported in Figure 6B. In order to better compare among them
590 the results, Figure 6C reports a section of Figure 6B, focused on
591 the profiles obtained within 8 h after of the oral administration
592 of the powders. It can be observed that the free γ -indomethacin
593 powder induced a concentration peak in the rat bloodstream of
594 about $5 \mu\text{g}/\text{mL}$ 2 h after the administration. A similar profile
595 was obtained with mixtures 1 and 2, whereas mixture 3 was
596 characterized by a profile showing a peak concentration of
597 about $3.5 \mu\text{g}/\text{mL}$ 2 h after its administration.
598

599 The co-crystal 1 induced a concentration peak in the rat
600 bloodstream of about $5 \mu\text{g}/\text{mL}$ 30 min after the administration,
601 the same time required for co-crystal 3 to induce a
602 concentration peak of about $3 \mu\text{g}/\text{mL}$. The co-crystal 2 profile
603 was instead characterized by a peak lower than $2 \mu\text{g}/\text{mL}$
604 obtained between 1 and 2 h after the administration. In general,
605 the profiles of the co-crystals appeared characterized by a
606 decrease of indomethacin blood concentration within 4 h after
607 their administration with a rate lower than those observed
608 following free γ -indomethacin and the parent mixtures
609 administrations.

610 The AUC values of the profiles reported in Figure 6B were
611 employed for the calculation of absolute bioavailabilities (F) of
612 the solid formulations, reported in Table 2. In particular the 612

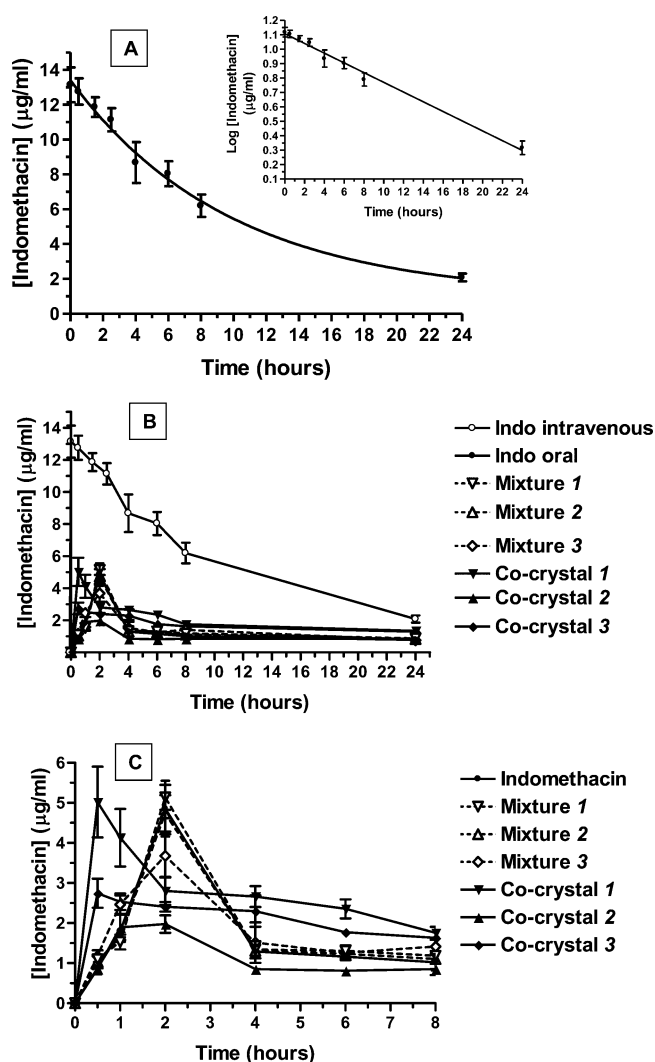


Figure 6. (A) Elimination profile of indomethacin after 0.90 mg infusion to rats. The elimination followed an apparent first order kinetic, confirmed by the semilogarithmic plot reported in the inset ($n = 8$, $r = 0.983$, $P < 0.0001$). The half-life of indomethacin was calculated to be 8.94 ± 0.38 h. (B) Blood indomethacin concentrations ($\mu\text{g/mL}$) after intravenous infusion (iv) or oral administration of 0.90 mg dose to rats within 24 h. The oral formulations were constituted by the sieved powders of free γ -indomethacin, its co-crystals, and the parent mixtures. (C) Detailed blood indomethacin concentrations ($\mu\text{g/mL}$) after oral administration of 0.90 mg dose to rats within 8 h. All data reported in the figure are expressed as the mean \pm SD of four independent experiments.

613 free γ -indomethacin powder was characterized by an F value of
 614 $23.5 \pm 0.8\%$, not statistically dissimilar ($P > 0.05$) from those of
 615 mixtures 1, 2, and 3. The co-crystals 1 and 3 were characterized
 616 by significantly higher ($P < 0.001$) F values than free γ -
 617 indomethacin ($37.7 \pm 1.5\%$ and $33.58 \pm 0.59\%$, respectively),
 618 while, co-crystal 2 induced a relatively small, but significant (P
 619 < 0.001), decrease of bioavailability with respect to the powder
 620 of the free drug (F value = $20.1 \pm 0.9\%$).

621 ■ DISCUSSION

622 Co-crystallization, by enhancing BCS class II API solubility, has
 623 been proposed as a new strategy to increase drug
 624 bioavailability.^{9–17} However, experimental evidence about the
 625 effects of the co-crystals on the permeation of APIs across

intestinal barriers and on intestinal epithelial barrier integrity is 626
 not reported in the literature. These studies should be relevant 627
 as the disruption of intestinal epithelial tight junctions has two 628
 undesirable consequences: unwanted substances such as 629
 endotoxins are allowed into the body, and depolarization of 630
 cells may be promoted.^{32,33} Moreover, the regulatory status 631
 regarding the use of co-crystals in pharmaceutical products 632
 appears still unsettled, it being necessary to clarify whether the 633
 co-crystal would be defined as a physical mixture or as a new 634
 chemical entity requiring full safety and toxicology testing.^{7,8} In 635
 the attempt to contribute to clarify these aspects, we have 636
 chosen indomethacin as a model BCS class II API and 637
 compared its properties with those of three of its co-crystals 638
 along with their parent physical mixtures. To our knowledge, 639
 this type of study is absolutely novel, being not only focused on 640
 a systematic comparison among the behavior of powders 641
 constituted by the pure API, its co-crystals, and their parent 642
 mixtures, but also involving the analysis of the API permeation 643
 across an *in vitro* intestinal barrier model. 644

The dissolution studies were first performed in a 200 mM 645
 phosphate buffer, pH 7.4. The relatively high ionic strength of 646
 this buffer was necessary to maintain the stability of the pH 647
 value during the dissolution processes.¹⁹ As already described, 648
 we have observed that the dissolution profile of indomethacin 649
 was not altered by the presence of the co-crystallizing agents in 650
 the form of physical mixtures with the API, whereas significant 651
 changes were observed by the dissolution of the co-crystals. 652
 This behavior is consistent with the different crystal packing 653
 forces due to the different intermolecular interaction patterns of 654
 the considered crystals as described in Results. These 655
 differences are reflected by the different thermal behavior of 656
 the indomethacin and its co-crystals. In particular, the enthalpy 657
 data for γ -indomethacin and co-crystal 3 differ by about 39 kJ/
 658 mol, as previously reported;¹⁹ in this case the higher lattice
 659 energy of 3 is related to a solubility higher than that of the pure
 660 indomethacin, similarly as it happens with co-crystal 1. It is
 661 known³⁴ that the ideal solubility depends on the melting
 662 temperature and enthalpy of the solute; such behavior, 663
 however, only applies to specific cases, such as polymorphs. 664
 On the contrary, melting point, along with related enthalpy
 665 values, “has often been shown to be a poor parameter to judge
 666 aqueous solubilities of co-crystals”,³⁵ indicating that the co-
 667 crystal solubility is dependent on more than a single factor. 668

A qualitative concordance between the API dissolution 669
 patterns in the 200 mM phosphate buffer and its absorption in 670
 the rat bloodstream after the oral administration of the powders 671
 has been observed. In particular, dissolution (Figure 4A) and
 672 bioavailability (Figure 6C) profiles of pure γ -indomethacin
 673 were similar to those of its physical mixtures with the co-
 674 crystallizing molecules; on the other hand either indomethacin
 675 solubility or its bioavailability was significantly increased by co-
 676 crystals 1 and 3, and weakly decreased by co-crystal 2. It is
 677 worth noting that, to allow a direct comparison among the
 678 powder constituted by the free drug, its co-crystals, and the
 679 parent mixtures, we intentionally decided to not follow the
 680 suitable formulation strategies suggested to improve the plasma
 681 levels of APIs orally administered as co-crystals.⁹ This can
 682 explain the relatively weak, although significant, changes of
 683 bioavailability induced by the co-crystallization observed in the
 684 present study. However, the accordance between dissolution
 685 and bioavailability profiles described above is in line with
 686 literature data concerning pharmaceutical co-crystals.^{10–17}
 687 Since this correlation does not provide any information on 688

689 the effective role of the co-crystals in influencing the API
690 absorption mechanisms across the intestinal barrier, we decided
691 to perform permeation experiments across NCM460 cell
692 monolayers. These studies are absolutely innovative for systems
693 involving pharmaceutical co-crystals and their parent mixtures.
694 Various cell monolayer models that mimic the human
695 intestinal epithelial barrier have been developed, providing ideal
696 systems for the rapid *in vitro* assessment of the intestinal
697 absorption of drug candidates. We have chosen the human
698 normal colonic epithelial NCM460 cells, their being an
699 immortalized, non-transformed cell line, derived from primary
700 cells of the normal human transverse colonic mucosa.²⁹ As
701 these cells are not of tumor origin nor transfected ones, they
702 retain more closely the physiological characteristics of the
703 normal human colon compared to the pathologically or
704 experimentally transformed cell lines. In this context, it is
705 worth noting that TEER developed by the NCM460 cells are
706 within the range reported for intact sheets of human colonic
707 mucosa.^{36,37} Furthermore, the lipophilic nature of indomethacin
708 enables the molecule to diffuse quickly and to get absorbed
709 completely through the intestinal membrane after oral
710 ingestion, resulting as almost equally permeable in the colon
711 and small intestine.^{38,39}

712 The permeation studies were performed by glucose-enriched
713 PBS as dissolution medium of the indomethacin powder, the
714 concentration of 200 mM phosphate buffer being too high to
715 allow cell survival. Moreover, PBS represented the simplest
716 medium in which to dissolve indomethacin from its powders,
717 in order to study the permeation properties across NCM460 cells
718 in the absence of other interfering substances. It is indeed
719 known that simulated intestinal buffers can induce TEER
720 changes of the monolayers and have inhibitory activity toward
721 efflux transporters expressed on the cell membranes.⁴⁰ As
722 described above, the dissolution profiles in PBS of indomethacin
723 showed some marked differences with respect to the
724 patterns obtained in 200 mM phosphate buffer, attributable to
725 the PBS relatively weak buffering power.

726 The suspensions obtained by the introduction of the solid
727 powders containing indomethacin in the apical compartments
728 of the "Millicell" systems allowed us to simulate an oral
729 administration. The γ -indomethacin crystals appeared able to
730 maintain the integrity of the monolayer characterized by TEER
731 values around 180 $\Omega \cdot \text{cm}^2$. Moreover, a comparison of the
732 permeability values obtained in the absence and in the presence
733 of cell monolayer validated the ability of this preparation to
734 behave as a physiologic barrier. We have instead observed that
735 the physical mixture of indomethacin and saccharin induced a
736 drastic decrease of the TEER value of the monolayer, whose
737 cells appeared to lose completely their mutual contacts after 1 h
738 of incubation. Surprisingly, the incubation with the parent co-
739 crystal 3 allowed the integrity of the monolayer as well as of its
740 TEER value to be maintained, and induced an increase of
741 indomethacin permeation across the NCM460 cells, with
742 respect to γ -indomethacin crystals. These results appear
743 unexpected, it being currently believed that the co-crystal-
744 lization strategy should influence the dissolution properties of
745 an API, without inducing changes on its pharmacological
746 profile.^{11,18} Conversely, the opposite effects observed on
747 NCM460 cells using mixture 3 and co-crystal 3 indicate that
748 APIs can have highly different biological behavior dependent on
749 the type of powder (a physical mixture or a co-crystal) from
750 which they are dissolved. A similar aspect was also observed for
751 co-crystal 1 and its parent mixture 1. In particular we have

observed that co-crystal 1 induced a drastic decrease of the
TEER value of the monolayer, whose cells appeared completely
separated after 1 h of incubation. The permeation profile of
indomethacin dissolved from co-crystal 1 showed indeed the
highest values with respect to all other cases, probably due to
both the loss of the barrier effect of the monolayer and the
increased dissolution of the API. Surprisingly, the incubation
with the parent physical mixture 1 did not induce any changes
on the monolayer integrity, as evidenced by unaffected TEER
value after 1 h of incubation. Moreover, the permeation profile
of indomethacin dissolved from this mixture was the same as
that obtained with solid γ -indomethacin. The phenomenon of
the different biological behavior of the powders does not,
however, amount to a systematic rule. Indeed, no significant
differences between γ -indomethacin and co-crystal 2 or mixture
2 were observed, as far as the integrity of the monolayer and
API permeation profile is concerned.

Several previous studies described API gastrointestinal
absorption by using cell lines.^{41,42} To the best of our
knowledge, however, none of them have been performed
with the employment of co-crystals. At present, on the basis of
our results we would venture to guess that the molecules
constituting the co-crystal in some way could retain in solution
some of the interactions formed in the solid state. If it be so, the
resulting molecular aggregations, although transient, could
interact with the proteins responsible for drug transport and for
the integrity of the cellular layers with different mechanisms
with respect to the molecules coming from pure crystals'
dissolution. It is worth noting that the affinity of APIs for
proteins is induced by specific and concerted weak interactions.
Thus, the different dissolution mechanisms at molecular level of
an API, dissolving from a co-crystal or from its parent physical
mixture, may have important different effects on the proteins of
biological systems.

CONCLUSIONS

To the best of our knowledge this is the first study
demonstrating different effects induced by co-crystals and
their parent physical mixtures on a biologic system, findings
that could raise serious concerns about the use of co-crystal
strategy to improve API bioavailability without performing
appropriate investigations. In this case co-crystal 1 was found to
induce a drastic decrease of the TEER value of NCM460 cell
monolayers, whereas its parent mixture did not evidence any
effect. On the other hand, the physical mixture of saccharin and
indomethacin was able to induce a drastic decrease of the
TEER value of NCM460 monolayers, whereas its parent co-
crystal 3 did not evidence any effect on the integrity of the
monolayers, being anyway able to increase the permeation of
indomethacin across the monolayers. On the basis of the
present experimental data we can only hypothesize the
reason(s) for these phenomena, but it is clearly evidenced
that the biological effects of a co-crystal and its parent mixture
can be drastically different, even if this is not to be taken as a
general rule. Indeed, any difference was registered by our
permeation measurements between co-crystal 2 and its parent
physical mixture on NCM460 cell monolayer.

Our results seem to open new perspectives about the
application of pharmaceutical products containing co-crystals.
New and appropriate investigations appear therefore necessary
in order to evaluate the potential new applications and the
potential damaging effects of pharmaceutical co-crystals.

813 ■ ASSOCIATED CONTENT

814 ● Supporting Information

815 Experimental details and crystallographic analysis. This material
816 is available free of charge via the Internet at <http://pubs.acs.org>.

817 ■ AUTHOR INFORMATION

818 Corresponding Author

819 *Department of Chemical and Pharmaceutical Sciences,
820 University of Ferrara, via Fossato di Mortara 19, I-44121,
821 Ferrara, Italy. Phone: +39-0532-455274. Fax: +39-0532-
822 455953. E-mail: dla@unife.it.

823 Notes

824 The authors declare no competing financial interest.

825 ■ REFERENCES

- 826 (1) Dressman, J.; Reppas, C. Drug Solubility: How To Measure It,
827 How To Improve It. *Adv. Drug Delivery Rev.* **2007**, *59*, 531–532.
828 (2) Morissette, S. L.; Soukasene, S.; Levinson, D.; Cima, M. J.;
829 Almarsson, O. Elucidation of Crystal form Diversity of the HIV
830 Protease Inhibitor Ritonavir by High-Throughput crystallization. *Proc.*
831 *Natl. Acad. Sci. U.S.A.* **2003**, *100*, 2180–2184.
832 (3) Heinz, A.; Strachan, C. J.; Gordon, K. C.; Rades, T. Analysis of
833 Solid-State Transformations of Pharmaceutical Compounds Using
834 Vibrational Spectroscopy. *J. Pharm. Pharmacol.* **2009**, *61*, 971–988.
835 (4) Schultheiss, N.; Newman, A. Pharmaceutical Cocrystals and
836 Their Physicochemical Properties. *Cryst. Growth Des.* **2009**, *9*, 2950–
837 2967.
838 (5) Jones, W.; Motherwell, W. D. S.; Trask, A. V. Pharmaceutical
839 Cocrystals: An Emerging Approach to Physical Property Enhance-
840 ment. *MRS Bull.* **2006**, *31*, 875–879.
841 (6) Remenar, J. F.; Morissette, S. L.; Peterson, M. L.; Moulton, B.;
842 MacPhee, J. M.; Guzman, H. R.; Almarsson, O. Crystal Engineering of
843 Novel Cocrystals of a Triazole Drug with 1,4-Dicarboxylic Acids. *J.*
844 *Am. Chem. Soc.* **2003**, *125*, 8456–8457.
845 (7) Brittain, H. G. Cocrystal Systems of Pharmaceutical Interest:
846 2010. *Cryst. Growth Des.* **2012**, *12*, 1046–1054.
847 (8) Brittain, H. G. Cocrystal Systems of Pharmaceutical Interest:
848 2011. *Cryst. Growth Des.* **2012**, *12*, 5823–5832.
849 (9) Childs, S. L.; Kandi, P.; Lingireddy, S. R. Formulation of a
850 Danazol Cocrystal with Controlled Supersaturation Plays an Essential
851 Role in Improving Bioavailability. *Mol. Pharmaceutics* **2013**, *10*, 3112–
852 3127.
853 (10) Hickey, M. B.; Peterson, M. L.; Scoppettuolo, L. A.; Morissette,
854 S. L.; Vetter, A.; Guzman, H.; Remenar, J. F.; Zhang, Z.; Tawa, M. D.;
855 Haley, S.; Zaworotko, M. J.; Almarsson, O. Performance Comparison
856 of a Cocrystal of Carbamazepine with Marketed Product. *Eur. J.*
857 *Pharm. Biopharm.* **2007**, *67*, 112–119.
858 (11) Jung, M. S.; Kim, J. S.; Kim, M. S.; Alhalaweh, A.; Cho, W.;
859 Hwang, S. J.; Velaga, S. P. Bioavailability of Indomethacin-Saccharin
860 Cocrystals. *J. Pharm. Pharmacol.* **2010**, *62*, 1560–1568.
861 (12) Weyna, D. R.; Cheney, M. L.; Shan, N.; Hanna, M.; Zaworotko,
862 M. J.; Sava, V.; Song, S.; Sanchez-Ramos, J. R. Improving Solubility
863 and Pharmacokinetics of Meloxicam via Multiple-Component Crystal
864 Formation. *Mol. Pharmaceutics* **2012**, *9*, 2094–2102.
865 (13) Smith, A. J.; Kavuru, P.; Wojtas, L.; Zaworotko, M. J.; Shytle, R.
866 D. Cocrystals of Quercetin with Improved Solubility and Oral
867 Bioavailability. *Mol. Pharmaceutics* **2011**, *8*, 1867–1876.
868 (14) McNamara, D. P.; Childs, S. L.; Giordano, J.; Iarriccio, A.;
869 Cassidy, J.; Shet, M.S.; Mannion, R.; O'Donnell, E.; Park, A. Use of a
870 Glutaric Acid Cocrystal To Improve Oral Bioavailability of a Low
871 Solubility API. *Pharm. Res.* **2006**, *23*, 1888–1897.
872 (15) Bak, A.; Gore, A.; Yanez, E.; Stanton, M.; Tufekcic, S.; Syed, R.;
873 Akrami, A.; Rose, M.; Surapaneni, S.; Bostick, T.; King, A.;
874 Neervannan, S.; Ostovic, D.; Koparkar, A. The Co-Crystal Approach
875 To Improve the Exposure of a Water-Insoluble Compound: AMG 517
876 Sorbic Acid Co-Crystal Characterization and Pharmacokinetics. *J.*
877 *Pharm. Sci.* **2008**, *97*, 3942–3956.

- (16) Stanton, M. K.; Kelly, R. C.; Colletti, A.; Langley, M.; Munson, 878
E.J.; Peterson, M. L.; Roberts, J.; Wells, M. Improved Pharmacoki- 879
netics of AMG 517 through Co-Crystallization Part 2: Analysis of 12 880
Carboxylic Acid Co-Crystals. *J. Pharm. Sci.* **2011**, *100*, 2734–2743. 881
(17) Zheng, W.; Jain, A.; Papoutsakis, D.; Dannenfels, R. M.; 882
Panicucci, R.; Garad, S. Selection of Oral Bioavailability Enhancing 883
Formulations during Drug Discovery. *Drug Dev. Ind. Pharm.* **2012**, *38*, 884
235–247. 885
(18) Bethune, S. J.; Schultheiss, N.; Henck, J. O. Improving the Poor 886
Aqueous Solubility of Nutraceutical Compound Pterostilbene through 887
Cocrystal Formation. *Cryst. Growth Des.* **2011**, *11*, 2817–2823. 888
(19) Basavoju, S.; Bostrom, D.; Velaga, S. P. Indomethacin-Saccharin 889
Cocrystals: Design, Synthesis and Preliminary Pharmaceutical 890
Characterization. *Pharm. Res.* **2008**, *25*, 530–541. 891
(20) Otwinowski, Z.; Minor, W. Processing of X-Ray Diffraction 892
Data Collected in Oscillation Mode. In *Methods in Enzymology*, *276*, 893
Macromolecular Crystallography, Part A; Carter, C. W., Jr., Sweet, R. 894
M., Eds.; Academic Press: New York, 1997; pp 307–326. 895
(21) Altomare, A.; Burla, M. C.; Camalli, M.; Cascarano, G.; 896
Giacovazzo, C.; Guagliardi, A.; Moliterni, A. G.; Polidori, G.; Spagna, 897
R. SIR97: A New Tool for Crystal Structure Determination and 898
Refinement. *J. Appl. Crystallogr.* **1999**, *32*, 115–119. 899
(22) Sheldrick, G. M. *SHELXL97, Program for Crystal Structure* 900
Refinement; University of Göttingen: Göttingen, Germany, 1997. 901
(23) Farrugia, L. J. WinGX Suite for Small-Molecule Single-Crystal 902
Crystallography. *J. Appl. Crystallogr.* **1999**, *32*, 837–838. 903
(24) Burnett, M. N.; Johnson, C. K. *ORTEP III. Report ORNL-6895*; 904
Oak Ridge National Laboratory: Oak Ridge, TN, USA, 1996. 905
(25) Dalpiaz, A.; Paganetto, G.; Pavan, B.; Fogagnolo, M.; Medici, A.; 906
Beggiato, S.; Perrone, D. Zidovudine and Ursodeoxycholic Acid 907
Conjugation: Design of a New Prodrug Potentially Able To Bypass the 908
Active Efflux Transport Systems of the Central Nervous System. *Mol.* 909
Pharmaceutics **2012**, *9* (4), 957–968. 910
(26) Artursson, P.; Karlson, J. Correlation Between Oral Absorption 911
in Humans and Apparent Drug Permeability Coefficients in Human 912
Intestinal Epithelial (Caco-2) Cells. *Biochem. Biophys. Res. Commun.* 913
1991, *175*, 880–885. 914
(27) Pal, D.; Udata, C.; Mitra, A. K. Transport of Cosalane, a Highly 915
Lipophilic Novel Anti-HIV Agent, across Caco-2 Cell Monolayers. *J.* 916
Pharm. Sci. **2000**, *89*, 826–833. 917
(28) Raje, S.; Cao, J.; Newman, A. H.; Gao, H.; Eddington, N. D. 918
Evaluation of the Blood-Brain Barrier Transport, Population 919
Pharmacokinetics, and Brain Distribution of Benzotropine Analogs 920
and Cocaine Using in Vitro and in Vivo Techniques. *J. Pharmacol. Exp.* 921
Ther. **2003**, *307*, 801–808. 922
(29) Kistenmacher, T. J.; Marsh, R. E. Crystal and Molecular 923
Structure of an Antiinflammatory Agent, Indomethacin, 1-(*p*- 924
Chlorobenzoyl)-5-methoxy-2-methylindole-3-acetic Acid. *J. Am.* 925
Chem. Soc. **1972**, *94*, 1340–1345. 926
(30) Wardell, J. L.; Low, J. N.; Glidewell, C. Saccharin, Redetermined 927
at 120 K: a Three-dimensional Hydrogen-Bonded Framework. *Acta* 928
Crystallogr. **2005**, *E61*, o1944–o1946. 929
(31) Moyer, M. P.; Manzano, L.; Merriman, R.; Stauffer, J.; Tanzer, 930
L. R. NCM460, a Normal Human Colon Mucosal Epithelial Cell Line. 931
In Vitro Cell. Dev. Biol.: Anim. **1996**, *32*, 315–317. 932
(32) Laurent-Puig, P.; Blons, H.; Cugnenc, P. H. Sequence of 933
Molecular Genetic Events in Colorectal Tumorigenesis. *Eur. J. Cancer* 934
Prev. **1999**, *8* (Suppl. 1), S39–S47. 935
(33) Rao, R. K.; Seth, A.; Sheth, P. Recent Advances in Alcoholic 936
Liver Disease I. Role of Intestinal Permeability and Endotoxemia in 937
Alcoholic Liver Disease. *Am. J. Physiol.* **2004**, *286*, G881–G884. 938
(34) Yalkowsky, S. H. *Solubility and Solubilization in Aqueous Media*; 939
Oxford University Press: New York, Copyright American Chemical 940
Society, 1999. 941
(35) Roy, L.; Lipert, M. P.; Rodriguez-Hornedo, N. Co-crystal 942
Solubility and Thermodynamic Stability. In *Pharmaceutical Salts and* 943
Co-crystals; Wouters, J., Quere, L., Eds.; Royal Society of Chemistry: 944
Cambridge, 2012; pp 247–279. 945

- 946 (36) Sahi, J.; Nataraja, S. G.; Layden, T. J.; Goldstein, J. L.; Moyer,
947 M. P.; Rao, M. C. Cl⁻ Transport in an Immortalized Human Epithelial
948 Cell Line (NCM460) Derived from the Normal Transverse Colon.
949 *Am. J. Physiol.* **1998**, *275* (4 Part 1), C1048–1057.
- 950 (37) Liu, Z. H.; Shen, T. Y.; Zhang, P.; Ma, Y. L.; Moyer, M. P.; Qin,
951 H. L. Protective Effects of *Lactobacillus Plantarum* against Epithelial
952 Barrier Dysfunction of Human Colon Cell Line NCM460. *World J.*
953 *Gastroenterol.* **2010**, *16*, 5759–5765.
- 954 (38) ElShaer, A.; Hanson, P.; Mohammed, A. R. A Novel
955 Concentration Dependent Amino Acid Ion Pair Strategy to Mediate
956 Drug Permeation using Indomethacin as a Model Insoluble Drug. *Eur.*
957 *J. Pharm. Sci.* **2014**, *62*, 124–131.
- 958 (39) Ehrhardt, C.; Kim, K. J. *Drug Absorption Studies: In Situ, In Vitro*
959 *and In Silico Models*; Springer: New York, 2008.
- 960 (40) Ingels, F.; Defermec, S.; Destexhe, E.; Oth, M.; Van den
961 Mooter, G.; Augustijns, P. Simulated Intestinal Fluid as Transport
962 Medium in the Caco-2 Cell Culture Model. *Int. J. Pharm.* **2002**, *232*,
963 183–192.
- 964 (41) Le Ferrec, E.; Chesne, C.; Artusson, P.; Brayden, D.; Fabre, G.;
965 Gires, P.; Guillou, F.; Rousset, M.; Rubas, W.; Scarino, M. L. In Vitro
966 Models of the Intestinal Barrier. The Report and Recommendations of
967 ECVAM Workshop 46. European Centre for the Validation of
968 Alternative Methods. *Altern. Lab. Anim.* **2001**, *29*, 649–668.
- 969 (42) Scaldaferrri, F.; Pizzoferrato, M.; Gerardi, V.; Lopetuso, L.;
970 Gasbarrini, A. The Gut Barrier: New Acquisitions and Therapeutic
971 Approaches. *J. Clin. Gastroenterol.* **2012**, *46*, S12–S17.